Embedding lipid nanodispersions in matrices: preparation of solid dosage forms with high lipid content and structural investigations using atomic force microscopy

Fabian C. Herrmann , Nicole Hofmann , Fiona Haslacher , Denise Steiner

PII: S0928-0987(25)00277-5
DOI: https://doi.org/10.1016/j.ejps.2025.107279
Reference: PHASCI 107279

To appear in: *European Journal of Pharmaceutical Sciences*

Received date: 7 August 2025
Revised date: 5 September 2025
Accepted date: 16 September 2025

Please cite this article as: Fabian C. Herrmann , Nicole Hofmann , Fiona Haslacher , Denise Steiner , Embedding lipid nanodispersions in matrices: preparation of solid dosage forms with high lipid content and structural investigations using atomic force microscopy, *European Journal of Pharmaceutical Sciences* (2025), doi: https://doi.org/10.1016/j.ejps.2025.107279

Embedding lipid nanodispersions in matrices: preparation of solid dosage forms with high lipid content and structural investigations using atomic force microscopy

Fabian C. Herrmann[1], Nicole Hofmann[1], Fiona Haslacher[2], Denise Steiner[3]

[1]University of Münster, Institute for Pharmaceutical Biology and Phytochemistry, PharmaCampus, Corrensstrasse 48, 48149 Münster/Germany

[2] Eberhard Karls University Tübingen, Department of Pharmaceutical Technology, Auf der Morgenstelle 8, 72076 Tübingen/Germany

[3]University of Münster, Institute of Pharmaceutical Technology and Biopharmaceutics, PharmaCampus, Corrensstrasse 48, 48149 Münster/Germany

Keywords:

Orodispersible film; spray drying; lipid-containing powders; lipid nanoparticles; nanoemulsions; tristearin; particle shape; particle modification; AFM

Abstract

Lipid nanodispersions are a promising formulation strategy for improving the bioavailability of drugs that are poorly water-soluble but highly lipophilic. Since patients prefer solid dosage forms, further processing of the liquid formulations is necessary. In order to expand the range of applications for drugs formulated in lipid nanodispersions, a high lipid content is required in the solid dosage forms. The aim of the current study was to determine the maximum loading capacity of lipid nanoemulsions and nanosuspensions by embedding the dispersions into orodispersible films and lipid-containing powders using spray drying. Atomic force microscopy enabled an assessment of the particle arrangement in the solid dosage forms and identified a stack-like orientation of the platelet-shaped triglyceride particles when embedded in orodispersible films. During the preparation of the powders by spray drying, a random particle arrangement was achieved, which was caused by the melting of the lipid particles during processing. Furthermore, atomic force microscopic images showed that tristearin particles in the metastable α-modification can exist in elongated to platelet-like shape traced back to the particle formulation and preparation process. The highest loading capacity in the solid dosage forms was achieved when the lipid nanodispersions were embedded in a film-forming matrix of PVA, resulting in lipid contents of up to 47 wt.%. Similar high lipid contents were achieved when lactose was used as the matrix material during spray drying.

1. Introduction

The number of newly developed but poorly water-soluble drug candidates is steadily increasing, with these poor physical properties mainly attributable to high lipophilicity or/and highly stable crystal lattices of the substances [1]. A lipid-based formulation approach is a particularly promising strategy for drugs with high lipophilicity [2, 3]. Thereby, a major advantage of lipid nanocarriers is their improved drug safety. This is because the lipids used are physiological and, thus, tolerated by the human organism, furthermore, no toxic co-solvents or pH adjustments are required to improve the solubility of the drug [4]. The food-effects that frequently occur when poorly water-soluble drugs are administered perorally could

also be reduced when these substances were formulated in lipid-based carriers [5, 6]. Two carrier systems that are well known in literature are lipid nanoemulsions and lipid nanosuspensions. A difference between them is the physical state of the used lipids, which additionally affects the localization of the embedded drugs. While in emulsions the drug molecules are located both on the surface and in the core of the lipid droplets, often enabling a higher drug load, in suspensions the drug mainly accumulates on the surface of the crystalline solid lipids [7]. Regardless of the carrier system used, however, further processing into solid dosage forms is advantageous, as these are better accepted by patients than liquid dosage forms [8].

A further processing of the lipid nanodispersions into a solid form aims to maintain the particle sizes of the nanocarriers even after redispersion of the dosage forms in water. Recent studies have shown that this poses a challenge, as lipid nanoemulsions, for example, tend to coalescent easily [9, 10]. Therefore, sufficient stabilization of the droplets and a supportive matrix material to prevent coalescence during processing are essential. It was shown that good particle size preservation can be achieved when the emulsions are embedded in a matrix e.g. by spray drying [11, 12], whereas coalescence occurred when the droplets were embedded in a film-forming HPMC matrix to prepare orodispersible films (ODFs) [13]. Lipid nanosuspensions are based on crystalline lipid particle that do not coalesce. This makes them a somewhat simpler system when formulations are to be further processed into solid dosage forms. It has been shown that high lipid contents can be achieved in ODFs, although these depended on the type of lipid embedded in the HPMC matrix [14].

In order to improve the usability of these nanocarriers for less potent and higher-dose drugs, high lipid loads of various carrier systems and different types of lipids in solid dosage forms are essential. Visualization of the nanoparticulate dosage forms could be beneficial in order to better understand the embedding of the nanodispersions in solid matrices. Currently, techniques such as scanning electron microscopy (SEM) or transmission electron microscopy (TEM) are the gold standard for nanoparticular systems. Although these techniques can achieve high resolution, they require a vacuum and complex sample preparation. This can lead to artifacts and changes in the original structure of the samples and is also time-consuming and resource-intense [15, 16]. Oil-containing nanoemulsions in particular are very challenging to measure, so cryo-electron microcopy often has to be used [17]. Atomic force microscopy (AFM) is a promising alternative technique for these nanoparticulate formulations. It can be operated under ambient conditions and requires little sample preparation. Recent studies have shown that various types of lipid carrier systems can be successfully visualized using AFM. Since AFM is the only microscopic technique delivering precise z-axis data, the gradual scanning of the sample with a cantilever can provide additional information such as particle sizes or surface roughness as well as mechanical properties could be obtained [16, 18]. In recent studies, solid lipid nanoparticles made from materials such as Compritol® 88 ATO [19] and lipid nanoemulsions consisting, for example, of medium-chain triglycerides (MCT) [20] were measured and visualized. AFM has also been used to visualize lipid nanodispersions in gelatin films [21] or gel matrices made of polyacrylic acid, xanthan, or hyaluronic acid [22]. In addition, nanoparticulate systems embedded in ODFs, such as nanoparticles of the drug buspirone hydrochloride [23] or mesoporous silica nanoparticles loaded with prednisolone [24], were characterized using AFM.

This study focuses on the embedding of high contents of different lipid nanodispersions into solid dosage forms and the visualization of the embedded carriers using AFM to identify the orientation of the nanoparticular systems depending on the chosen preparation technique. Various matrix materials are being evaluated to enable a successful embedding of different

types of lipid carriers into the solid matrices without loss of their nanoparticulate properties. For this purpose, ODFs and powders prepared by spray drying were selected for closer investigation, as their preparation differs fundamentally in terms of process parameters such as drying temperature and time, but similar matrix materials can be used. This study aimed to evaluate the embedding behavior of drug-free nanoparticulate lipid carrier systems using two different techniques in order to identify carrier formulations and matrix materials that are suitable for high lipid loading, while the additional embedding of drug molecules is part of a future study.

2. Material and Methods

2.1 Materials

Lipid nanodispersions were prepared from the liquid oil MCT (medium chain triglycerides, Miglyol® 812, Caesar&Loretz, Hilden, Germany) and the solid lipids trimyristin (Dynasan 114), tripalmitin (Dynasan 116) and tristearin (Dynasan 118; all IOI Oleo, kind gifts, Hamburg, Germany). The dispersions were stabilized using the additives polyvinyl alcohol (PVA, Kuraray Poval 4-88; Kuraray Europe Hattersheim, Germany), hydroxypropyl methyl cellulose (HPMC, Tylopur 606; Shin-Etsu SE Tylose GmbH, Wiesbaden, Germany; kind gift from Harke Pharma, Germany) and the surfactant sodium dodecyl sulphate (SDS, Carl Roth, Karlsruhe, Germany). Lipid nanodispersions were embedded in the following matrices: lactose (GranuLac® 200, Meggle, kind gift, Wasserburg am Inn, Germany), HPMC (Tylopur 606) and PVA EG-18P (for ODFs, GOHSENOL; Mitsubishi Chemical Group, Tokyo, Japan; kind gift from Harke Pharma, Germany) and PVA 4-88 (for spray drying; Kuraray Europe Hattersheim, Germany). The ODFs also contained the plasticizer glycerol (Carl Roth, Karlsruhe, Germany).

2.2. Methods

2.2.1 Preparation of lipid nanodispersions

Lipid nanoemulsions and nanosuspensions were prepared by high-pressure homogenization with a lipid content of 10 wt.%. An electrosteric stabilization was applied using 5 wt.% HPMC or PVA, and 0.5 wt.% SDS in the lipid nanodispersion. The emulsification process was performed at room temperature for MCT or at approx. 10 °C above the melting temperature of the solid lipids. Prior to emulsification a pre-emulsion was prepared from the liquid (melted) lipid and the aqueous solution containing the stabilization additives. The homogenization was performed with an Ultra Turrax (IKA-Werke, Staufen im Breisgau, Germany) for 2 min at 13,000 rpm (resolution per minute). The high-pressure homogenization was performed afterwards with two different devices of an EmulsiFlex C3 (Avestin, Ottawa, CA/USA) at 1500 bar for 10 cycles. Particle crystallization of the lipid nanosuspensions was done by cooling the formulations to room temperature, trimyristin formulations were crystalized at 5 °C for 30 min. All formulations were stored at room temperature for no longer than two weeks before being used for further processing.

2.2.2 Embedding of lipid nanodispersions in orodispersible films

Lipid nanodispersions were embedded in two different film-forming matrices: HPMC and PVA. Different processes were used to prepare ODFs containing liquid oil and solid lipid.

To prepare MCT-containing ODFs with the film-forming matrix PVA, the nanoemulsions were first heated to 60 °C and the PVA powder was added to the emulsion while the formulation was

stirred on a magnetic stirrer until the PVA was dissolved. The emulsion was then cooled to room temperature while stirring. The amount of PVA in the formulation was adjusted depending on the final lipid content in the dried ODFs, varying between 8 wt.% and 52 wt.%. At lipid contents in the films of 35 wt.% and less, water was added to the formulations to achieve viscosities of the film-casting formulations between 1 and 5 Pas (at a shear rate of 100 1/s, measured with a rotational viscometer). Finally, 6.7 wt.% of glycerol referred to PVA was added, and the formulation was stirred for at least another hour.

When the MCT emulsion was embedded in an HPMC film-forming matrix, a dissolver (PG-001; Thierry, Stuttgart, Germany) with a 30 mm dissolver disc was used to dissolve the HPMC powder in the emulsion at room temperature. During the addition of the powder, the formulation was stirred at 750 rpm, then the speed was increased to 2530 rpm for 20 min. Afterwards glycerol was added (33 wt.% referred to HPMC) and the mixture was dispersed for further 10 min at 3030 rpm. If required, water was added to achieve viscosities of the film-casing formulations between 1 Pas and 5 Pas (at a shear rate of 100 1/s).

Lipid nanosuspensions were embedded in the PVA matrix by mixing the suspension with an aqueous solution of 10 wt.% PVA and 1 wt.% glycerol. The solution was first stirred for at least 8 h to remove air bubbles and then mixed with the lipid nanosuspension in different ratios to obtain the desired lipid content in the dried films (10 to 50 wt.%). The film-casting mass was homogenized using an Ultra Turrax for 1 min at 10,000 rpm.

All lipid-containing film-casting masses were degassed overnight before further processing into films. The MCT-containing films were cast onto a PET (polyethylene terephthalate) foil at a casting height of 800 μm at 25 mm/s using a ZAA 2300 (Proceq, Schwerzenbach, Switzerland) automatic film applicator. The film-casting masses in which lipid nanoparticles were embedded, were poured into a glass Petri dish (9 g formulation, diameter 10 cm). All films were dried overnight at room temperature and stored in plastic bags at room temperatures until characterization.

2.2.3 Embedding of lipid nanodispersions in a matrix by spray drying

In addition to the preparation of ODFs, the lipid nanodispersions were embedded in a lactose, PVA or HPMC matrix by spray drying. For this purpose, a Büchi B-191 (Büchi AG, Flawil, Switzerland) was used in a co-current air flow mode. The dryer was operated with a peristaltic pump with a flow rate of 3.4 mL/min and a two-fluid nozzle with an orifice diameter of 0.7 mm. The air volume flow was set at approx. 35 m^3/h, the spray gas flow was approx. 667 L/h. A high-performance cyclone was used for particle separation. Samples were dried at an inlet temperature T_{in} of 150 °C. Before spray drying the formulations, the dryer was first heated up and then water was sprayed for approx. 5 min.

The spray formulation was prepared by mixing the lipid nanodispersion with matrix/SDS solution shortly before drying. An aqueous lactose/SDS solution with 5 wt.% lactose and 0.5 wt.% SDS was used for embedding the dispersion in lactose. For PVA and HPMC, the polymer concentration was 2.5 wt.% and 0.25 wt.% SDS in the aqueous solution.

For all formulations, the lipid content in the dried powders was between 10 wt.% and 55 wt.%. The powders were stored in a glass vial at room temperature until characterization.

2.3 Characterization of lipid nanodispersions and solid formulations

2.3.1 Particle size analysis

Depending on the resulting particle sizes, the formulations were measured using laser diffraction (LD) or photon correlation spectroscopy (PCS). A LA-960 (Horiba Scientific, Kyoto, Japan) was used for the LD particle size measurements. The device was equipped with a glass cuvette and the samples were diluted with distilled water before measurement. A refractive index of 1.46 was assumed for the lipids (absorption index of 0.01) and 1.33 for water. All samples were measured in triplicate and the volume distributions were calculated according to the Mie theory. Particle sizes are expressed as x_{50} or x_{90} values in this study. In order to evaluate the widths of the size distributions, the span was calculated according to equation 1.

$$span = \frac{x_{90} - x_{10}}{x_{50}} \qquad \text{(Equ. 1)}$$

PCS measurements were performed with a Zetasizer Nano ZS (Malvern Instruments, Malvern, United Kingdom). The intensity-weighted mean diameter (z-average) and the polydispersity index (PdI), as a value of the distribution width, were determined at an angle of 173°. The samples were measured at 25 °C in triplicate, 60 s each, after an equilibration time of 180 s. The lipid nanodispersions (10 μL) were diluted in 3 mL water immediately before the particle size analysis. The mean values and the standard deviations were calculated for each measurement. Due to very small standard deviations and for better clarity of the graphs, these were not displayed in the graphs.

2.3.2 Determination of particle sizes from solid formulations and redispersibility index

To obtain the size of the particles or droplets after redispersing the solid dosage forms in water, the ODFs (size 1 cm^2) and powders (approx. 5 mg) were first dissolved in 1.0 mL of water for two hours. Depending on the formulation, further sample dilution with purified water was required prior to particle size measurement.

In order to compare the particle sizes of the nanodispersions before further processing into solid forms with the sizes after redispersion, the redispersibility index (RdI) was calculated according to equation 2 [25, 26]. Drying and redispersion was considered successful if the RdI value was less than or equal 1.2, indicating a maximum 20 % increase in particle sizes after redispersion.

$$RdI = \frac{particle\ size\ of\ redispersed\ formulation\ in\ water\ [nm]}{particle\ size\ of\ original\ nanodispersion\ [nm]} \qquad \text{(Equ. 2)}$$

2.3.3 Differential scanning calorimetry

Differential scanning calorimetry (DSC) was used to analyze the polymorphic state of the lipid nanoparticles prepared from solid lipids. The measurements were performed with a DSCQ2000 (TA Instruments, Eschborn, Germany). Samples were weighed into 40 μL aluminum crucibles and cold sealed after loading. For the analysis of liquids, 13 μL sample were used, while for solid formulations, approx. 5 mg of the spray-dried powders or three round ODF samples with a diameter of 4 mm were stacked on top of each other, according to [14], also resulting in a total sample weight of approx. 5 mg. The samples were generally analyzed at a heating rate of 10 °C/min from 25 °C to 85 °C. To additionally assess the physical state of the trimyristin dispersions in the spray-dried powders, the samples were cooled from 20 °C to 4 °C at a cooling rate of 10 °C/min. The suspensions and powders were measured directly after preparation (0 d) as well as after one (1 d) and twelve days (12 d).

2.4 Atomic force microscopy

The prepared ODFs were subsequently transferred into BEEM capsules (size 00) and embedded in UV-curable epoxy resin (Monocure 3D Rapid epoxy resin, Monocure, Sidney, Australia). In order to prepare a surface suitable for atomic force microscopy (AFM) measurements of the ODFs, the embedded epoxy blocks were sectioned on an ultramicrotome (Ultracut E, Leica Microsystems GmbH, Wetzlar, Germany), employing freshly prepared glass knives, leading to a considerably flat surface of the sectioned ODFs in the epoxy block, allowing direct AFM imaging in air under ambient conditions.

Spray dried powders were also prepared for nanoscopic AFM imaging by embedding into UV-curable epoxy resin. Initially, an amount of approx. 50 mg of powder preparation was thoroughly mixed with 100 µL of epoxy resin inside the tip of a size 00 BEEM capsule. Subsequently, epoxy resin was added up to 75 % of the capsule height. The block was then directly polymerized using UV light, removed from the BEEM capsules and ultra-sectioned as described above for the ODF preparations.

Lipid nanosuspensions were prepared for AFM imaging in air by applying 10 µL of stirred suspension on a freshly cleaved MICA disc and drying in the applied spot under continuous air flow (lab bench). The dried in spot was subsequently covered with around 100 µL of Aqua Millipore for 15 min. Finally, the water was rapidly removed and the sample dried again by pressurized air (hand bellows), allowing facile imaging of particles by AFM in intermittent contact mode.

AFM measurements were afterwards performed on the surfaces of the previously sectioned blocks and MICA discs, using a Bruker Dimension 3100 AFM (Bruker, Karlsruhe, Germany), equipped with a Nanoscope IIIa controller in intermittent contact mode in air under ambient conditions (HQ:NSC 14 Al BS cantilevers by µmasch, Sofia, Bulgaria). Analysis of AFM data was finally carried out employing the software Nanoscope Analysis 3.0 (Bruker, Karlsruhe, Germany).

2.5 Scanning electron microscopy

Scanning electron microscopy (SEM) images were taken of a selected ODF sample. A Helios G4 CX (FEI Deutschland GmbH, Frankfurt, Germany) was used to picture the particle arrangement of a film cross-section. The samples were prepared by sputtering with gold at 5 mA for 4 min and the images were then taken in a high vacuum at a voltage of 1.00 kV.

3. Results and Discussion

3.1. Embedding of lipid nanoemulsions in solid matrices

Lipid nanoemulsions embed the drug molecules both in the matrix and the droplet surface, but often do not have a high drug load due to the limited solubility of the drugs in the oil. However, in order to achieve high doses of drugs in a solid dosage form, high amounts of lipid must be embedded in the solid matrices, whereby the nanoparticulate properties of the lipid carrier systems should be retained after redispersion of the dosage form in water. Two different solid dosage forms are investigated in more detail in this study: ODFs and powders prepared by spray drying. While ODFs are prepared by dispersing the lipid carrier systems in film-forming

polymers and drying them for several hours at room temperature, water evaporation during spray drying takes place within a few seconds at high temperatures. Differences in the loading capacity of the various matrix materials and the arrangement of the droplets in the matrices are evaluated.

3.1.1 Lipid nanoemulsions embedded in ODFs

Recent studies indicated that the embedding of lipid nanoemulsions in ODFs is quite challenging due to the coalescence tendency of the lipid droplets [13]. It was shown that droplet stabilization with the surfactant SDS was not sufficient to prevent coalescence, regardless of whether the lipid nanocarriers are loaded with drug molecules or not. Therefore, the current study first evaluated the influence of droplet stabilization additives on coalescence tendencies during processing into ODFs. Instead of electrostatical droplet stabilization with SDS alone, the droplets were stabilized electrosterically by combining a polymer (HPMC or PVA) with the surfactant SDS. In addition to the most common film-forming polymer HPMC, PVA was additionally evaluated as matrix polymer.

Initial studies with the two different film-forming matrices show that when 24 wt.% lipid is embedded in the ODFs, the droplet coalescence indicated by the redispersibility index (RdI) after film redispersion is generally higher when HPMC is used as matrix material, regardless of the droplet stabilization (Table 1). While the stabilizing additives HPMC/SDS performed even worse than when the emulsion is stabilized with SDS alone, the combination PVA/SDS shows the most promising RdIs after film redispersion for both film-forming matrices. For a MCT formulation stabilized with PVA/SDS, no increase in droplet sizes is observed when the emulsion is embedded in the PVA matrix (RdI 1.0), and a RdI of 2.2 is obtained when HPMC was used as film-forming matrix.

Table 1: Influence of the droplet stabilization applied to the MCT emulsion and the film-forming matrix on the redispersibility of the droplets from the ODFs, indicated by the redispersibility index RdI; lipid content in all ODFs: 24 wt.%, droplet sizes measured using LD.

Droplet stabilization	**Film-forming matrix**	
	HPMC	**PVA**
	RdI [-]	RdI [-]
SDS	4.5*	---
HPMC/SDS	5.3	3.0
PVA/SDS	2.2	1.0

*calculated according to [13]

Based on these results, the additive combination PVA/SDS was selected to stabilize the MCT emulsion prior to embedding the droplets in the film-forming matrices HPMC or PVA, while the maximum possible lipid content in the ODFs was evaluated. All MCT emulsions used had droplet sizes (x_{50}) of approx. 120 nm before embedding in ODFs.

The results indicate that the trend already indicated (Table 1) continues when a wider range of lipid contents in the ODFs is examined (Figure 1). The droplet sizes of the MCT emulsions redispersed from the HPMC films and the width of the size distributions (span) are clearly higher than for the ODFs with a PVA matrix for all lipid contents investigated. It was found that droplet coalescence occurred in all films prepared with an HPMC matrix, even when the lipid content was reduced to 9 wt.%. Therefore, only the RdI value of the lowest lipid content with

RdI = 1.2 is considered acceptable. A clear increase in droplet sizes is obtained when the lipid content reached 30 wt.% or more, resulting in droplets larger than x_{50} = 1 μm. In addition to the droplet sizes, the width of the size distributions also increased, with bimodal size distributions and increasing x_{90} values being observed, particularly at lipid contents between 9 wt.% and 24 wt.%. A more promising embedding behavior was obtained when the film-forming matrix is PVA. Lipid contents of up to 45 wt.% can be realized without the size of the MCT droplets increasing after redispersion of the ODFs in water, indicated by RdI values of 1.0. A further increase in the lipid content up to 52 wt.% resulted in a slight increase in droplet sizes, with the RdI value only exceeding 1.2 at a lipid content of 52 wt.% (particle size increase approx. 60 nm). As for the span calculated from these size distributions, no significant increase is observed with increasing lipid contents. This shows that although the particle sizes increase with lipid contents of 45 wt.% and more, no bimodal droplet size distribution is obtained.

Despite these high lipid loads, all PVA-films could be easily removed from their liner and handled properly, with adequate mechanical properties as required by the European Pharmacopeia [27]. However, it should be noted that at lipid contents of 49 wt.% and above, an increasingly oily film was observed on the ODF surfaces over time (approx. 4 weeks). A MCT nanocarrier content of 47 wt.% in the PVA matrix is therefore considered to be the maximum possible for these dosage forms, whereby the RdI value of 1.1 is within the acceptable range for this formulation. These findings show that, within the scope of the current study, it was possible to embed a very high lipid content into the ODFs without causing droplet coalescence or other handling problems.

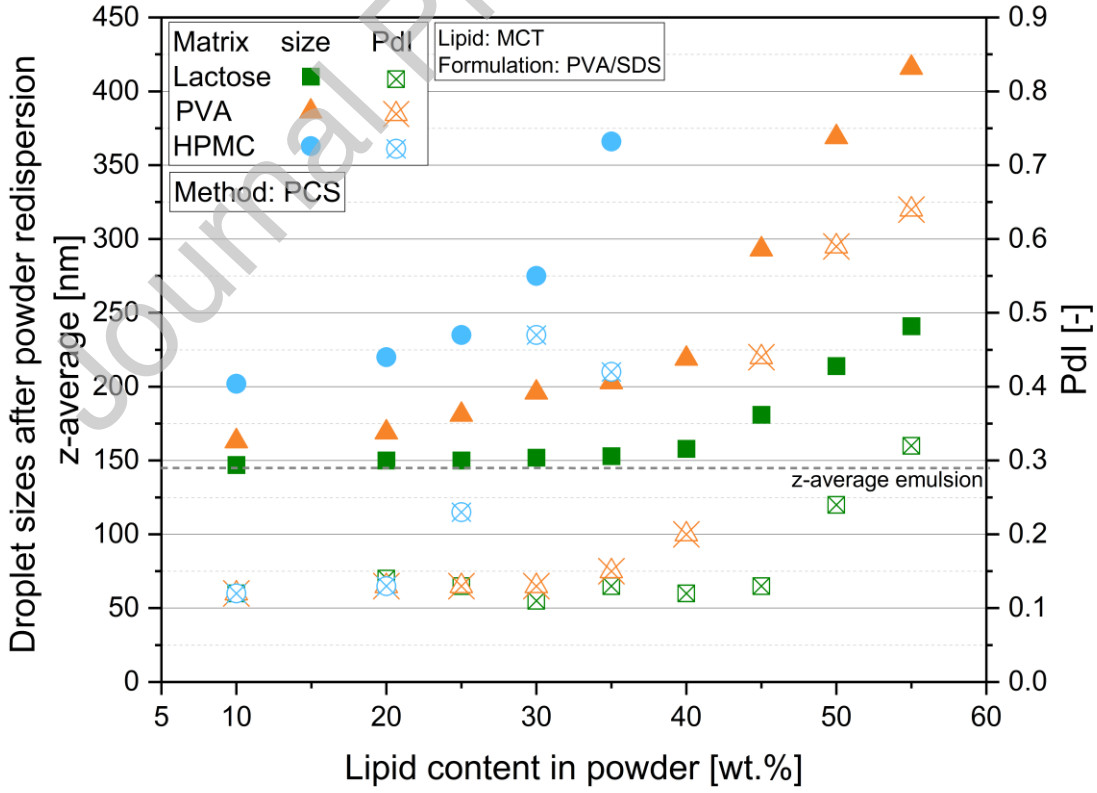

Figure 1: Droplet sizes and size distributions of MCT nanoemulsions redispersed from ODFs embedded in different film-forming matrices (HPMC and PVA) with different lipid contents; measured by laser diffraction.

The droplet size measurements after redispersion of the films indicate coalescence of the droplets when the emulsions were embedded in an HPMC matrix and almost no changes when PVA was used as matrix material. Nevertheless, these size measurements cannot provide information on whether the droplet coalescence occurred during the preparation process or whether the droplets coalesced when the films were redispersed in water for 2 h. While SEM imaging of an ODF loaded with a lipid liquid could only be performed in a cryo setup, this study uses AFM to investigate the structure of the ODFs in more detail, allowing sample measurement at room temperatures and ambient pressure.

First, AFM images of ODF cross-sections of the lipid-free HPMC and PVA films show structural differences between the matrix materials (Figure 2, top). While the surfaces of the PVA films appear smooth (Figure 2, top right), the films prepared of HPMC show a more structured surface (Figure 2, top left). These differences in appearance can be attributed to the different molecular structures of the polymers and their polymerization characteristics, which were visualized by the AFM. When lipid nanoemulsions were embedded in the ODFs (Figure 2, bottom), large voids can be seen in the cross-section of the films build up by the HPMC matrix. This proves that the droplets coalesced during the drying process, which took place at room temperature overnight. The films with a PVA matrix have a more branched structure, indicating the embedding of individual droplets in this matrix, which is confirmed by the droplet size measurements. It should be noted that the viscosities of the film-casting masses could have an impact on the droplet stability, as two different film-forming polymers were used. It was shown before that the coalescence time increases with higher viscosities of the continuous phase, which had a positive influence on the coalescence of the droplets [28]. While the film-forming polymers in this study were different, the film-casing formulations of the ODFs with a lipid content of 24 wt.% both had viscosities of approx. 3 Pas (at a shear rate of 100 1/s). It is therefore not assumed that the viscosity of the formulation influences the coalescence of the droplets in this case during the drying step. The differences in droplet stabilization during ODF drying are assumed to be caused by the composition of the molecules, which differ clearly in their molecular weight (HPMC approx. 330,000 g/mol, PVA approx. 31,000 g/mol), among other things.

It should be noted that the oil droplets themselves are not visible in the AFM images due to the sample preparation. Cutting the films before the measurement allows the droplets to run out, leaving holes in the matrix indicating their previous localization which were visualized. However, the AFM technique applied in this study made it possible to visualize the location of the oil droplets within the ODF structure under ambient conditions without time-consuming sample preparation, thus enabling conclusions to be drawn about the drying process.

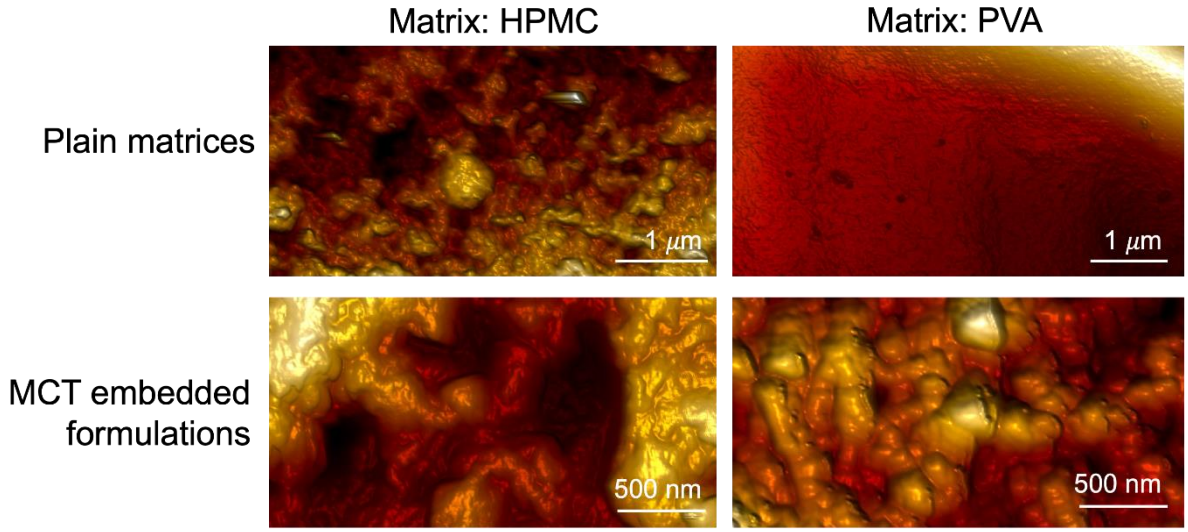

Figure 2: Atomic force microscopy image (3D display, enabling better comparability) of MCT emulsions stabilized with PVA/SDS embedded in an HPMC (left) and PVA matrix (right), lipid content in films 24 wt.%

Despite earlier studies, it was shown that a MCT emulsion could be successfully embedded in an ODF made of a PVA matrix. For films with an HPMC matrix, the AFM images indicated that the droplets coalesce during the drying process, which takes several hours during ODF preparation. To evaluate whether shorter drying times could positively influence the loading capacity of HPMC, spray drying was chosen as another drying technique for embedding lipid nanoemulsions in solid matrices.

3.1.2 Lipid nanoemulsions embedded in spray dried powders

Spray drying of a lipid nanocarrier is a different preparation technique compared to the film casting of ODFs. Although the formulations in this study are the same, the drying times as well as temperatures are particularly different. While the ODFs were dried for several hours at room temperature, the formulation is nebulized during spray drying and a hot air stream dries the droplets within seconds. In the following, the lipid nanoemulsions, like the ODFs, were embedded in a PVA or HPMC matrix in order to investigate the influence of the drying process used in more detail. In addition, lactose was chosen as a matrix material, as previous studies indicated good redispersibility of the nanoparticulate formulations after drying [12, 29]. To improve the wettability of the powders, the surfactant SDS was added to all formulations [12].

The embedding of different lipid contents in the matrices lactose, HPMC and PVA shows that the nanoparticular properties of the MCT emulsions (measured by PCS, z-average of starting emulsions between 145 nm and 150 nm) are best preserved when lactose is used as matrix material (Figure 3). Only slight particle size increases are obtained with lipid contents up to 40 wt.% in the powders. The width of the size distributions, indicated by the PdI, remain constant. At a lipid content of 45 wt.%, the particle sizes increase further to approx. 180 nm (RdI = 1.2), and at 50 wt.% and higher, a more pronounced coalescence of the droplets occurred, resulting in sizes above 200 nm and a clear increase in PdI.

It is also shown that the PVA matrix outperforms the HPMC matrix in terms of particle size preservation after redispersion of the solid forms. For powders containing PVA as a matrix, small increases in particle sizes were achieved at a MCT content in the powders of 25 wt.% or less (RdI ≤ 1.2). A further increase of the lipid content in the powders resulted in RdI values above 1.2. Regarding the PdIs of these measurements, it was found that at lipid contents of

35 wt.% and below, the size distributions are monomodal, determined by PdIs of maximum 0.15. With increasing droplet sizes well above 200 nm (40 wt.%) the PdI increases to 0.2, indicating a broader size distribution, while at lipid contents of 45 wt.% and above, a bi- or multimodal distribution was obtained, as indicated by PdIs above 0.4. With HPMC as matrix material, the largest droplet sizes were measured after powder redispersion in water. Particle sizes above 200 nm and a RdI value of 1.4 were already achieved for the lowest lipid content of 10 wt.%. At lipid contents of 30 wt.% and higher, PdIs of more than 0.4 were measured, which clearly indicates a bi- or multimodal size distribution and thus strong droplet coalescence. Lipid contents of 40 wt.% or higher were no longer considered in this study. HPMC as spray drying matrix was also used by Christensen et al., who embedded coconut oil emulsions. Their investigations on redispersibility revealed a maximum lipid content of up to 40 % in the dry powders, but they examined emulsions with clearly larges droplet sizes (x_{50} = 820 nm) [11], which makes a direct comparison not possible.

Differences in the performance of the various matrices could be caused by the different intrinsic dissolution rates (IDR) of the materials. Wewers et al. pointed out a correlation between IDR and RdI and showed that higher dissolution rates of the matrix materials resulted in lower RdI values when naproxen nanoparticles were processed into granules in a fluidized bed process [30]. They measured an IDR of 290 μg/cm^2·min for lactose, which is clearly higher than the IDR value of HPMC, which was determined to be approx. 19 μg/cm^2·min [31]. Furthermore, it was shown that the IDR value of PVA-containing formulations was higher than when HPMC was used as the matrix material [32], confirming the embedding capacities and resulting RdI values of the spray-dried formulations in the current study.

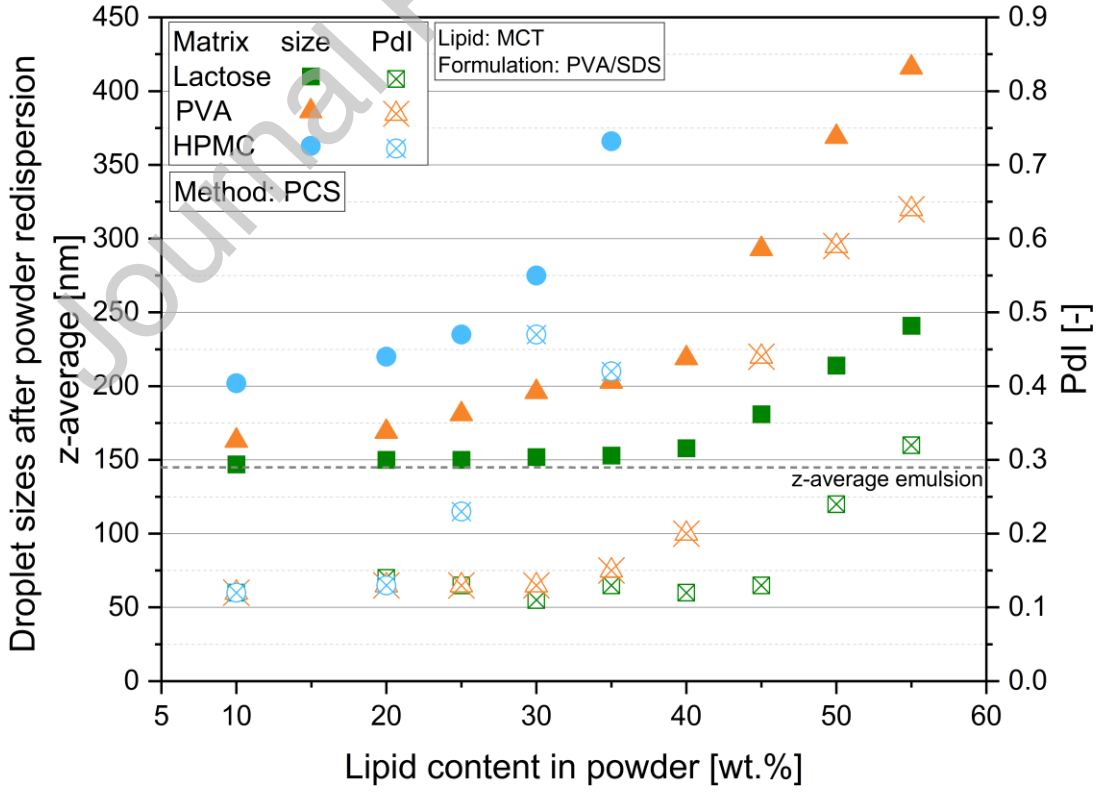

Figure 3: Evaluation of three matrix materials (lactose, PVA and HPMC) for the embedding of lipid nanoemulsions by spray drying. Samples measured by photon correlation spectroscopy, z-average and PdI are given.

Similar to the ODFs, AFM images were taken of the prepared powders, showing the embedded MCT nanoemulsion in a PVA and HPMC matrix with a lipid content of 25 wt.% (Figure 4). The images are comparable to those of the ODFs embedding the emulsions in the PVA film matrix. An uneven surface can be seen for both, showing the matrix in which the lipid droplets are embedded. Voids in the matrices indicate the location of the oil droplets in the dried powders. Size measurements confirm the droplet sizes of these samples to be less than 250 nm for both powders.

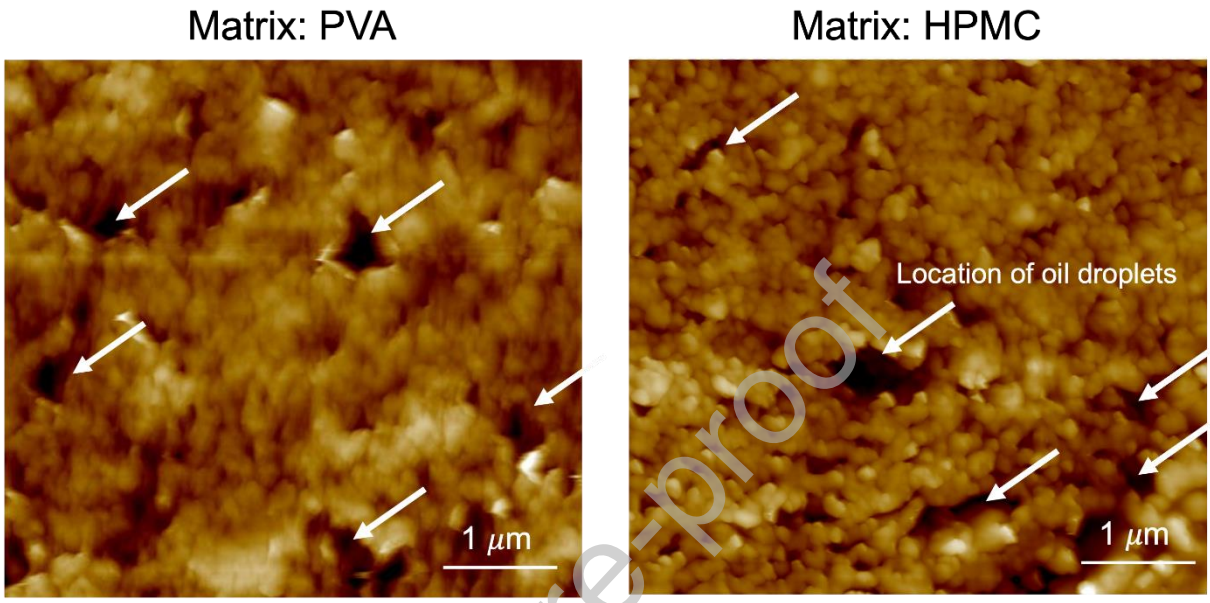

Figure 4: Atomic force microscopy images of powders embedding MCT emulsions stabilized with PVA/SDS by spray dried using PVA (left) and HPMC (right) as matrix material, lipid content in powders 25 wt.%, the arrows indicate the positions of droplets in the matrices.

When comparing the two different preparation techniques for embedding lipid nanoemulsions in matrices, it becomes clear that the droplet sizes can generally be preserved in both ODFs and spray-dried powders and that high lipid contents can be achieved in both cases. The highest lipid contents of up to 47 wt.% were achieved when lipid droplets are embedded in the ODFs with the film-forming polymer PVA. During spray drying, the PVA matrix material performed worse, with a maximum loading capacity of 25 wt.%. To enable high lipid contents lactose should be selected as the matrix material. It clearly performed best with acceptable RdI values for lipid contents up to 45 wt.%.

HPMC as a matrix material was identified to be not suitable for stabilizing lipid droplets during processing into solid dosage forms. Coalescence of the droplets was achieved with both preparation techniques, ODF casting and spray drying, regardless of the lipid content in the solid forms. At low lipid contents, the droplet sizes achieved appear to be in the broadest sense comparable, as for 20 wt.% MCT, for example, droplet sizes were 220 nm for spray-dried powders and 260 nm after redispersion from films. These results show that neither the direct drying of the formulation within seconds nor the shear forces to which the droplets are exposed during spray drying by atomization immediately before water evaporation prevent droplet coalescence. Previous studies have shown that for MCT emulsions with droplet sizes of approx. 3 μm, the atomization step reduced oil droplet sizes depended on the stabilizer systems selected. In all of these formulations, smaller particle sizes were obtained in the dried powders compared to the original emulsion, indicating a break-up of the oil droplets during atomization [33]. However, it has been shown that these results are not transferable to the nanoemulsions investigated in the current study. In general, it has been demonstrated that

high lipid contents are achievable with sufficient droplet stabilization and an adapted matrix formulation, regardless of the preparation techniques used.

3.2 Embedding of lipid nanosuspensions in solid matrices

The second carrier system under investigation in this study are lipid nanosuspensions. It has recently been shown that high lipid contents can be achieved by embedding tristearin in an HPMC-containing ODF matrix [14] or when spray drying these suspensions using lactose as matrix material [12]. The following sections build on these findings to improve the understanding of the embedding of the different platelet-shaped triglyceride particles (trimyristin, tripalmitin, tristearin) in various matrices using two preparation techniques and visualization by AFM. In addition, a focus was placed on the shape and modification of the tristearin particles embedded in the matrices.

3.2.1 Lipid nanosuspensions in ODFs

Recent studies indicated that particle size preservation after redispersion of ODFs in water strongly depends on the type of triglyceride embedded in an HPMC matrix. It was shown that tristearin particles allow a lipid loading of up to 50 wt.% (particle stabilization HPMC/SDS) with only a slight increase in particle sizes, while the maximum possible lipid loading was considerably lower for tripalmitin (40 wt.%) and trimyristin (29 wt.%) particles [14]. To investigate the influence of the matrix material in more detail, PVA was used as the matrix material in this study to assess whether the effects shown are caused by the embedded lipid or the film-forming polymer.

First, a suitable particle stabilization system was determined. A screening was carried out with the two polymers HPMC and PVA, both in combination with the surfactant SDS, to realize an electrosteric particle stabilization. Trimyristin particles with different lipid contents in the ODFs were used for this screening. It revealed that trimyristin particles stabilized with HPMC/SDS and embedded in the film-forming polymer PVA exhibit RdI values of 24.7 for a lipid content of 30 wt.% and higher with increasing lipid contents in the films (Table 2). However, almost no increase in particle size was observed when the particles were stabilized with PVA/SDS (RdI = 1.2) at a lipid content of up to 40 wt.%.

The stabilizing additives PVA/SDS were chosen for the following investigations of all lipid nanosuspensions. It should be noted that this stabilizer combination enables the stabilization of the metastable α-modification of the tristearin particles [34]. Thus, the tristearin particles were embedded in the matrix in α-modification, while tripalmitin and trimyristin particles transformed in the stable β-modification prior to ODF preparation. These differences have no influence on the processing of the suspensions into ODFs but are taken up again when particles were visualized in the film structure in section 3.2.3.

Table 2: Stabilization screening for trimyristin particles embedded in the film-forming matrix PVA by evaluation of RdI.

Lipid: trimyristin	**RdI [-]**	
Lipid content in ODF [wt.%]	Stabilizing additives HPMC/SDS	Stabilizing additives PVA/SDS
30	24.7	1.1
40	55.1	1.2

50	94.3	619.1

The embedding of tristearin, tripalmitin and trimyristin particles stabilized with PVA/SDS in a PVA matrix showed that after ODF redispersion only slight differences in particle sizes were achieved between the various lipid types (Figure 5). For all three types of lipid-containing films, almost no increase in particle sizes and no change in size distributions were observed up to a lipid content of 30 wt.% (all RdI < 1.2). The particle sizes increase slightly by a maximum of approx. 60 nm (x_{50}) when 40 wt.% lipid (RdI = 1.2 for trimyristin and tristearin, RdI = 1.5 for tripalmitin) was embedded in the film matrix, but the increased span, especially for tripalmitin, indicates a bimodal size distribution due to high x_{90} values and thus particle agglomeration. This phenomenon is even more pronounced at a lipid content of 45 wt.% with span values for all three lipids above 10. Clear particle agglomeration was achieved when 50 wt.% lipid particles were embedded in the PVA matrix, resulting in particles sizes larger than 100 μm (x_{50}).

These findings confirm a good embedding potential of the film-forming polymer PVA also for solid lipid nanoparticles. Slightly lower maximum loading capacities were achieved with the lipid particles in the matrix (40 wt.%) than with the MCT droplets (47 wt.%). It is assumed that this is due to the different shapes of the embedded lipid dispersions. While the MCT forms droplets, the specific surface area that enables interaction with other lipid droplets is lower than when the platelet-like particles are embedded in the matrix, which have a larger specific surface area. Furthermore, round particles are more likely to allow a close-packed arrangement, whereas platelet-shaped particles were previously assumed to form stacks above a critical particle concentration [35, 36], allowing less dense packing. A more detailed consideration of the arrangement of the particles in the film structure, also taking into account the different lipid modifications, is shown below (section 3.2.3).

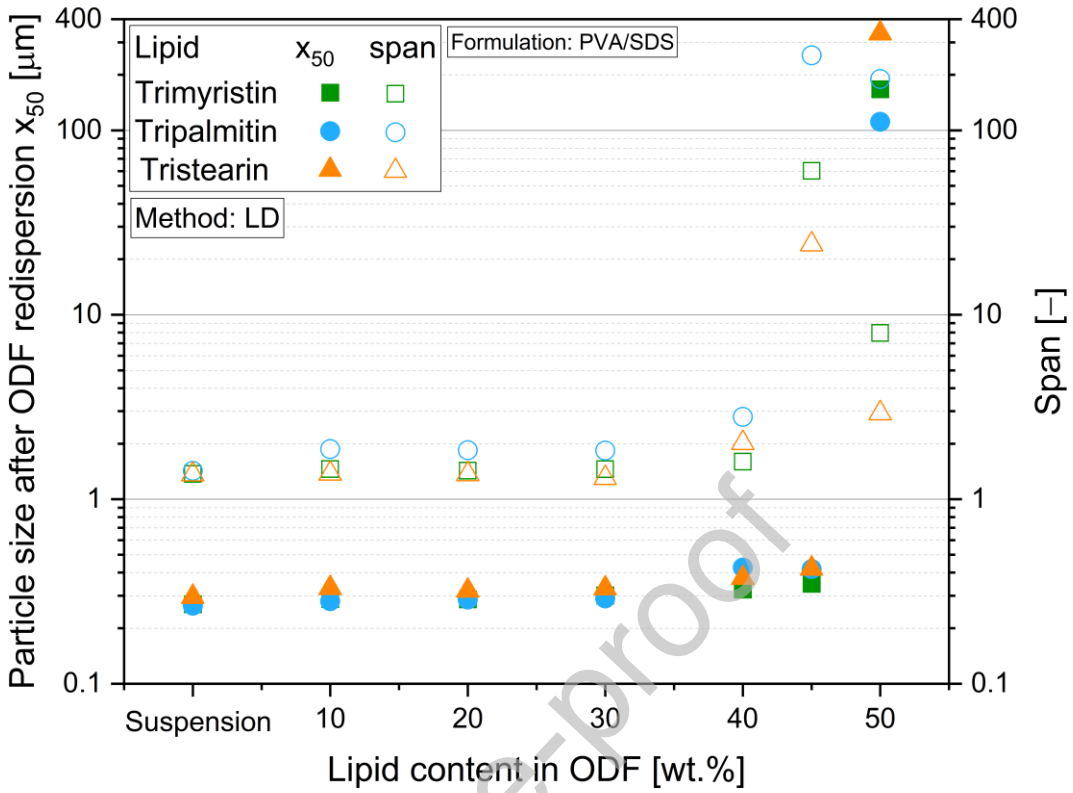

Figure 5: Particle sizes after ODF redispersion and span for the three different triglycerides trimyristin, tripalmitin and tristearin, embedded in the film-forming matrix PVA. The particles were formulated with PVA/SDS and the sizes were measured using lase diffraction.

The similar behavior of the triglycerides used show that the different chain lengths of the fatty acids of the triglycerides apparently have no influence on the loading capacities when PVA is used as matrix material. This suggests that very high lipid loadings can be realized in ODFs regardless of the nanodispersion used, and that the particle stabilization of the dispersions and the type of matrix material used mainly influence the loading capacity of the ODFs.

3.2.2 Lipid nanosuspensions in spray dried powders

When embedding lipid nanosuspensions in a solid matrix by spray drying, the heat to which the particles are exposed during processing have to be taken into account. It has already been shown that at a drying temperature T_{in} = 150 °C and a resulting outlet temperature of approx. 88 °C, tristearin particles melt during processing and recrystallize when the temperature falls below the crystallization temperature [12]. Whether this change in physical state has an influence on the embedding properties of the three investigated triglycerides and which matrix (lactose, HPMC and PVA) is best suited for high lipid loads is investigated below.

In order to evaluate the loading capacities of the matrices for the different triglycerides, the particle sizes were examined after powder redispersion (Figure 6). In general, it can be seen that the smallest particle sizes are achieved when all suspensions are embedded in the lactose matrix. Only minor differences in the particle sizes are obtained between the powders containing tristearin and tripalmitin. With a lipid content of up to 45 wt.%, the particle sizes increased by only approx. 30 nm compared to the suspensions (particle sizes approx. 170 nm);

RdI values for both lipids are 1.2. Powders with a lipid content of 50 wt.% and above showed clear particle agglomeration after redispersion in water. When embedding trimyristin particles, agglomeration occurs at lower lipid contents. The measurements show that a RdI value of 1.2 is achieved at a lipid load of 30 wt.% when particle sizes increase up to approx. 220 nm. A further increase in lipid content results in a strong increase in particle sizes and a RdI value of 4.5. One possible reason for the differences in the embedding behavior could be the physical state of the lipids embedded in the powders, as discussed below (Figure 7).

Similar to the results for the embedding of MCT droplets, HPMC also performed worst in the embedding of lipid particles. Although the lipid contents of the various triglycerides are only 10 wt.%, particle sizes increase to approx. 300 nm (RdI between 1.7 and 2.2) or more. Acceptable RdI values are achieved when tripalmitin and tristearin are embedded in the PVA matrix with a lipid content of 10 wt.%. At higher lipid contents, a gradual increase in particle agglomeration is observed.

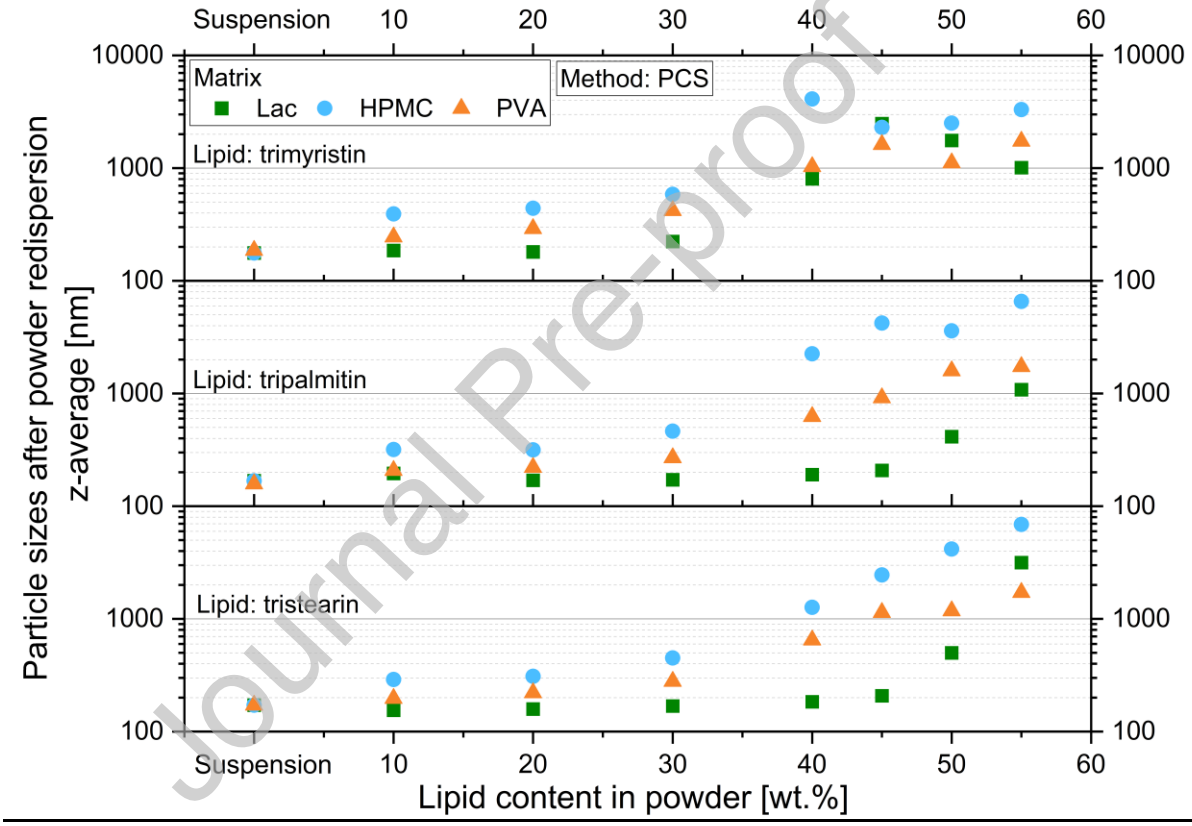

Figure 6: Evaluation of particle sizes after redispersion of powders embedding nanosuspensions of trimyristin, tripalmitin and tristearin in the matrices lactose, HPMC and PVA. Particles were stabilized using PVA/SDS and sizes were measured by photon correlation spectroscopy.

In general, similar trends are observed when embedding different triglyceride lipid nanodispersions in solid matrices, with lactose exhibiting the most efficient embedding capacity. This is attributed to efficient particle stabilization based on the similar polymer/surfactant combination for all formulations. However, the drying process has also to be taken into account. As mentioned above, the particles melt during spray drying. Due to the immiscibility of the lipids with the aqueous phase and the interfacial tension that occurs, it is assumed that the lipids form droplets or droplet-like shapes when they melt during spray drying. With an outlet temperature of approx. 88 °C, measured before the particles are

separated by the cyclone, lipid nanoparticles recrystallize after their embedding in the solid matrix in the storage vessel.

Unless tristearin and tripalmitin, trimyristin is known to form supercooled droplets. This means that the lipid crystallizes at temperatures below 10 °C and remains solid when warmed back to room temperature. In suspensions the lipid remains in liquid state if the formulation is cooled to room temperature after preparation [37]. In this study, all powders were cooled to room temperature after spray drying but not cooled further. While tristearin and tripalmitin crystallized clearly after the drying step, the trimyristin formulations embedded in the various matrices exhibited different behavior. To identify the physical state of the trimyristin embedded in the matrices, DSC measurements were performed (lipid content 30 wt.%), with two different setups being carried out: on the one hand, the samples were heated from 25 °C to 80 °C to evaluate the melting of the particles, which indicates the presence of crystallized trimyristin particles in the powders, and on the other hand, the samples were cooled from 20 °C to 4 °C. When trimyristin in liquid form is embedded in the powders, an exothermic event occurs at temperatures below 10 °C, indicating particle crystallization.

The DSC heating curve of the trimyristin suspension shows particle melting at an onset temperature of approx. 47 °C with an endothermic peak maximum at approx. 53 °C, which indicates tristearin particles in the stable β-modification in the suspension prior to spray drying (Figure 7, right). No thermal event is observed when the sample is cooled to 4 °C (Figure 7, left). An examination of the spray-dried powders revealed that the samples with the PVA and HPMC matrices show similar thermal behavior. While no crystallization is observed when the samples are cooled to 4 °C, the measurements demonstrate clear endothermic events, indicating that the particles crystallized immediately after preparation (0 d) without any additional cooling step. Various endothermic events are observed for these samples at different temperatures. The strongest melting signal is obtained at approx. 55 – 56 °C, which indicates particles in the stable β-modification. Compared to the suspension, a slight shift in the thermal maxima of the powders is observed. Similar trends were detected when lipid particles were embedded in ODFs, assuming they were caused by the solid matrix surrounding the particles [14]. At temperatures of approx. 32 °C, a smaller melting event is shown, indicating nanoparticles in the metastable α-modification [38]. Over the storage period of 12 d, it is observed that these peaks decrease, caused by the crystalline lattice of the particles transforming into the β-modification. Broader melting peaks at approx. 42 – 47 °C directly before the onset of the endothermic β-peaks, often described as shoulder (in suspensions), are assumed to be attributed to the metastable β'-modification [37]. This is supported by the fact that the peaks decrease over time, indicating further particle conversion to the stable β-modification.

The trimyristin particles embedded in the lactose matrix indicate a different behavior. Even after a storage period of 12 d, the cooling curves clearly show a crystallization peak with an onset of approx. 11 °C. However, endothermic events were also observed when the samples were heated to 80 °C. This shows that both liquid trimyristin droplets and solid particles are embedded in the powders. In terms of their storage behavior, an increase in melting enthalpy is observed, which is determined by the area under the curve of the DSC thermograms, while the enthalpy of the crystallization process decreases. Directly after preparation the share of solid particles in the powder was approx. 14 %, increasing to approx. 34 % within 12 d. DSC measurements also confirmed that all particles can be crystallized by cooling the powder to 5 °C for 1 h.

Previous studies have shown that the polymorphic status of triglyceride particles is influenced by parameters such as the additives chosen for particle stabilization and the cooling rate of the formulations [34, 39, 40]. While these parameters and the particle formulation (stabilization with PVA/SDS) were kept constant in the current study, it was found that the matrix materials can also influence the crystallization behavior of the trimyristin droplets in the dry powders. For the matrices PVA and HPMC, the trimyristin particles crystallized directly in the solid matrix, and no supercooled lipid droplets remain in the matrix, while the lactose matrix was initially able to stabilize most of the trimyristin droplets, which then slowly crystallized over time. In the context of amorphous solid dosage forms, PVA and HPMC are actually known as effective additives for preventing crystallization. Amorphous drugs, for example, have successfully been embedded in these matrices using techniques such as spray drying or vacuum drying [41-43]. In addition, tristearin nanoparticles were embedded in an HPMC-containing ODF matrix in the metastable α-modification, with only approx. 12 % of the particles transforming into the β-modification during a storage period of 6 months [14]. Although the glass transition temperature as criteria for characterizing amorphous solids is clearly higher for HPMC [41] than for amorphous lactose [44], complete droplet crystallization occurs immediately upon embedding in HPMC. Further investigations are necessary to identify the reasons for this behavior.

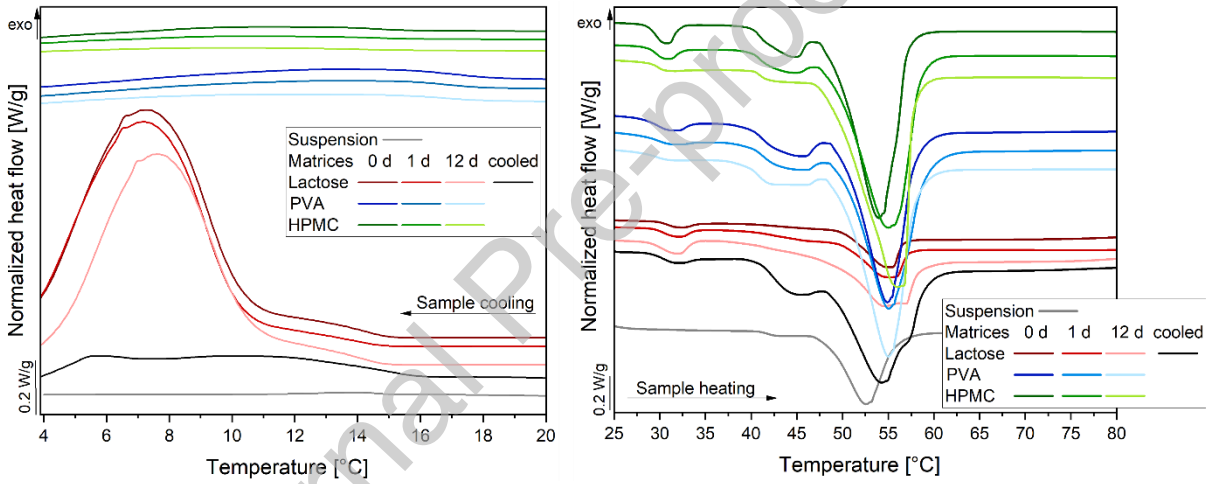

Figure 7: DSC thermograms of cooling (left) and heating (right) curves of a trimyristin suspension and spray-dried powders embedding trimyristin dispersions. Trimyristin was loaded into three different matrices (lactose, PVA and HPMC) and stored for up to 12 d.

3.2.3 Structure analysis of lipid particles in solid matrices

The analysis of the shape of triglyceride particles in various modifications has already been carried out by several groups. It is known that triglycerides can exist in different polymorphs, the metastable α- and β'-forms, which transform to the stable β-modification. In nanoparticles, this transformation is accelerated but, PVA as a stabilizing agent has been identified to improve the stabilization of the α-modification. However, storage temperatures above 5 °C and shorter-chain triglycerides such as trimyristin lead to a faster rearrangement of the crystal lattice [38]. The stabilization of the formulations in this study was performed with PVA/SDS, resulting in tristearin particles that were present in the α-modification for such a long time that they could be embedded in all formulations in the metastable modification. In the following, the form of the tristearin particles embedded in ODFs and spray dried powders (matrix material lactose) is first closer investigated.

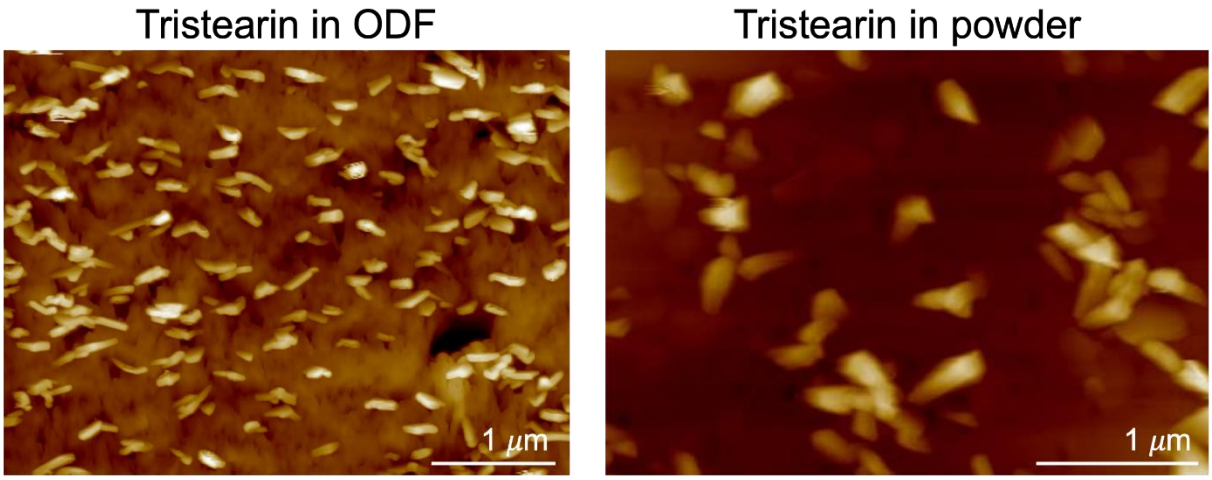

Figure 8: Atomic force microscopy images of tristearin particles embedded in an ODF (lipid content 40 wt.%, left) and spray dried powder (lipid content 25 wt.%, right).

Figure 8 displays tristearin particles embedded in an ODF (cross-section, left) and spray-dried powder (right). The images show particles embedded in a solid matrix, with both images displaying particles with an elongated to platelet-like shape. It has previously been shown in literature that the shape of triglyceride particles can vary dependent on their modification. While particles in the β-modification were platelet-shaped [2, 45], no general statement could be made for the particles in the α-modification. Various studies have shown that the shapes can vary depending on the cooling rate, storage conditions, and stabilization additives, ranging from (almost) spherical [35, 46, 47] to a more polyhedral, irregular shape [40, 48] or mixtures of circular as well as rectangular particles [38]. In general, the particles in the α-modification were found to be rounder than the platelet-like β-particles. If these findings are applied to the particles displayed in Figure 8, it can be assumed that they are embedded in the β-modification in the solid matrices. These findings were unexpected, as the particles in the starting suspension are in α-modification, as indicated by an endothermic peak at approx. 54 °C (Figure 9). Since the ODFs were prepared and dried at room temperature, no changes in the particle modification were assumed. During spray drying, the particles presumably melt and recrystallize into the α-modification upon cooling in the storage vessel. A closer look at the solid dosage forms was performed using DSC. To enable the assignment of the various possible melting peaks, a second tristearin nanosuspension, which had been stabilized with HPMC/SDS and stored for several months [12], was measured, whereby the melting temperature of the particles in the β-modification was determined to be approx. 67 °C. The DSC thermograph of the spray-dried powder clearly shows that the embedded tristearin particles are in the α-modification, as evidenced by the single endothermic melting event at approx. 54 °C. For the ODF sample a major melting peak displays the presence of particles in the α-modification. However, upon further heating of the sample, another endothermic and an exothermic event are observed. These are attributed to the crystallization performance previously observed for triglycerides and caused by the characterization method [34]. The exothermic event at approx. 59 °C indicates the crystallization of a small share of the previously melted lipid particles into the β-form. These particles melt again when the measuring temperature reaches approx. 67 °C. To determine the original share of particle in the β-modification, the enthalpy of the thermic event at approx. 67 °C (particles in β-modification) is subtracted from the endothermic event [34], indicating that 99.8 % of the particles embedded in the ODF are in α-modification.

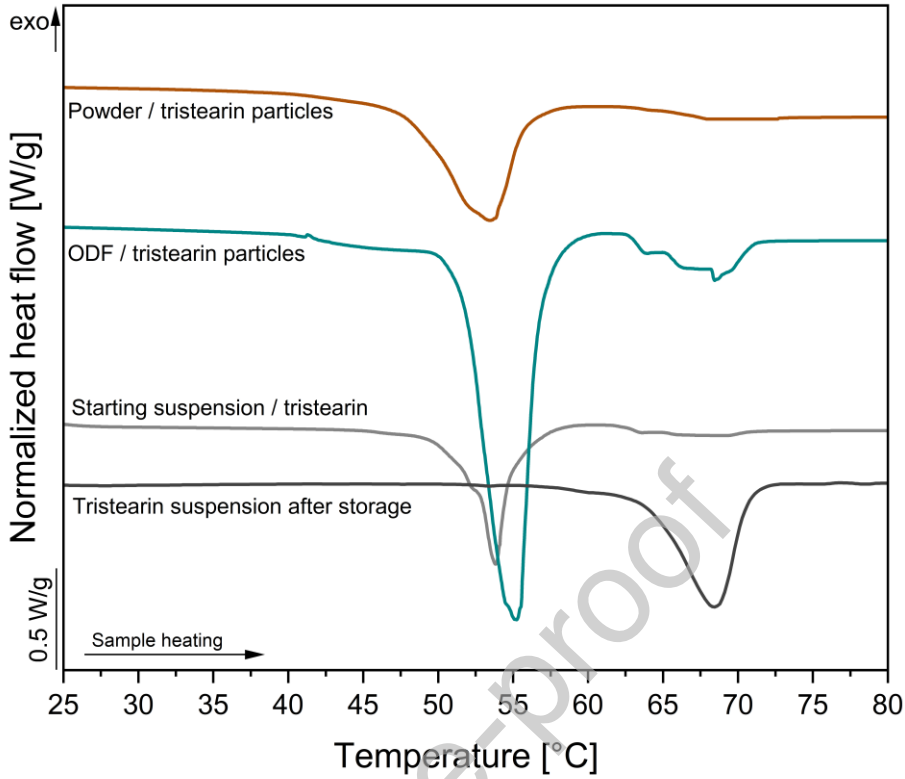

Figure 9: DSC heating curves of tristearin suspensions, ODF (lipid content 40 wt.%) and spray dried powder (lipid content 25 wt.%).

Contrary to previous assumptions regarding the shape of tristearin particles in the α-modification, this study shows that the elongated to platelet-like particles are in the α-polymorphic form. To confirm these results, additional SEM images of the cross-section of the ODF (Figure 10) were taken. The SEM images confirm the AFM measurements (Figure 8, left), displaying particles in platelet-like shape in the ODF matrix.

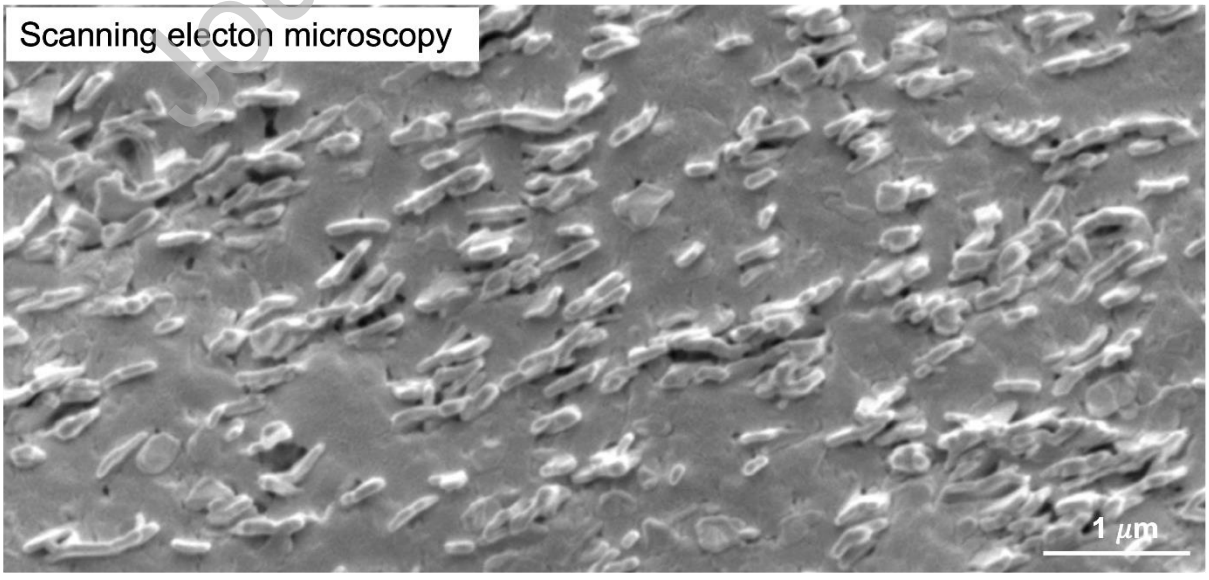

Figure 10: Scanning electron microscopy image of tristearin nanoparticles embedded in ODF, lipid content 40 wt.%.

Due to the fact that the ODFs were prepared at room temperature, it was assumed that the particle shape and modification had not changed, so AFM was used to identify the shape of the tristearin particles in the starting suspension present in the α-modification (Figure 11). The images show individual lipid particles (right) and two particles that were measured as examples in terms of their length and height (left). Although tristearin particles appear round at first glance, closer examination of the lengths and heights of the particles reveal a platelet-like shape. Because AFM measurements are enabling the highly precise determination of z-axis data (resolution around 0.1 nm), the subsequent analysis of 3D particle morphology can be carried out with unrivaled accuracy. Depending on the measurement lines drawn, the particles are between 80 nm and 150 nm long. The AFM measurements show a flat particle surface with a height between 10 nm and 30 nm, which does not indicate a spherical particle shape. This demonstrates that in the current study, the shape of the tristearin particles in the α-modification is not round or spherical, but rather elongated to platelet-like when stabilized with PVA/SDS, suggesting a new particle shape that could be formed by the tristearin particles in the metastable modification.

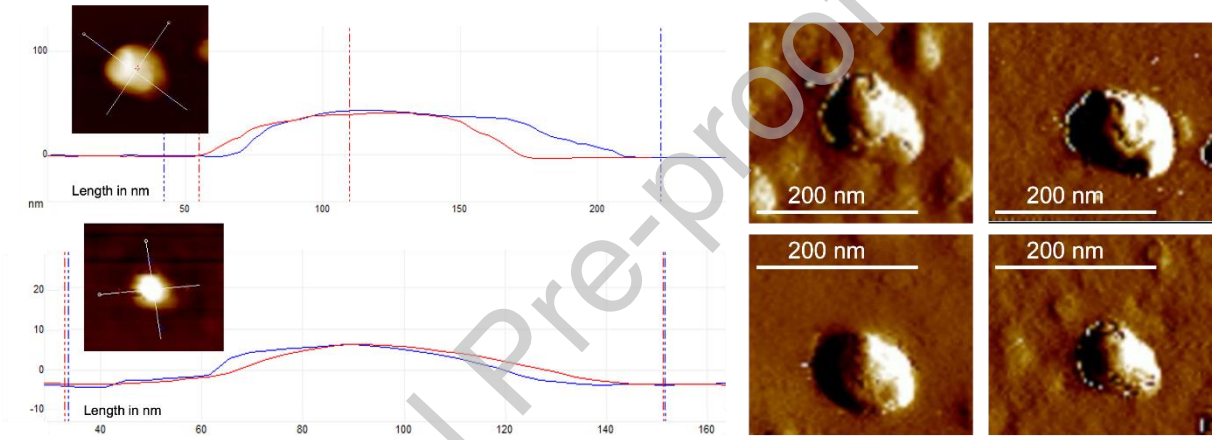

Figure 11: Atomic force microscopy images show single tristearin particles in α-modification (right) and the profiles of two selected particles indicating their length and height (left).

The reasons for these shapes are assumed to be caused by the stabilizing additives used during emulsification and the crystallization conditions of the particles. It has previously been shown that the cooling rate - slowly to room temperature or quickly from melt to 5 °C - resulted in different arrangements of the tripalmitin molecules when glycocholate was used as stabilizer. This resulted in different particle shapes, which were spherical when cooled rapidly and clearly more irregular when cooled slowly at room temperature [40]. Similar observations were made for tristearin dispersions using phospholipids as emulsifier [48]. With regard to the suspension examined in this study, the more irregular particle shapes are assumed to be due to, on the one hand, the slow cooling of the tristearin suspensions to room temperature, as was the case with the starting suspension after preparation. Although the tristearin particles melt during spray drying [12], they are collected in a vessel after being removed from the hot air stream and slowly cooled to room temperature, which could also enable the formation of elongated to platelet-like particles. On the other hand, it is assumed that the stabilization principal using a polymer and a surfactant influenced the shape of the crystallized particles.

Finally, the arrangement of the particles in the matrix is examined in more detail, with trimyristin-containing ODFs and powders (Figure 12) being considered as examples in addition to the tristearin-containing formulations (Figure 8). It becomes apparent that differences between the various preparation techniques are evident, while a similar embedding behavior is observed regardless of the type of triglyceride particles, all in platelet-like shape. The lipid

particles embedded in the ODF matrix indicate a particle orientation. They appear to be aligned in one direction and form a stack-like structure that developed during the very slow water evaporation overnight at room temperature, allowing the particles to rearrange themselves in the film-forming matrix. This confirms the findings of Schmiele et al. [49] and Gehrer et al. [35] who showed that platelet-shaped particles form nematically ordered domains above a critical particle concentration, which was received during the drying process of the ODFs. In contrast, no uniform structure is observed for the particles embedded in the matrix by spray drying. This is caused by the melting of the lipid particles during the drying process and the recrystallization after the water has evaporated from the sample. Since platelet-like shapes are observed for the lipid particles despite the embedding in the solid matrix, it can be assumed that the matrix does not influence the particle shape. However, this suppresses particle arrangement during drying, resulting in an unstructured particle distribution in the solid matrices.

These differences in particle arrangement could be one of the reasons why higher lipid contents were achieved in ODFs compared to spray-dried powders when PVA was chosen as matrix material. However, this behavior does not explain why the loading capacity of the platelet-like triglyceride particles is similar to that of MCT droplets when embedded in the lactose matrix and requires further investigation.

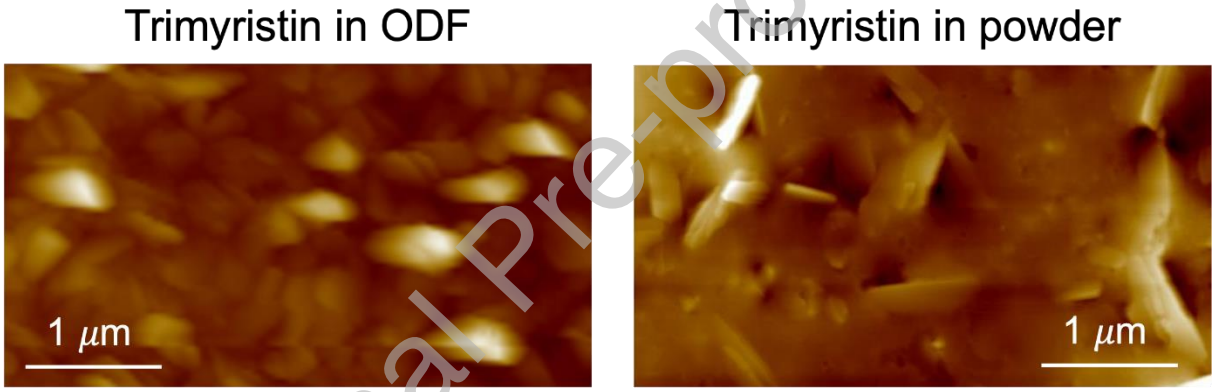

Figure 12: Atomic force microscopy images of trimyristin particles embedded in an ODF (lipid content 40 wt.%, left) and in a lactose matrix by spray drying (lipid content 25 wt.%, right)

4. Conclusion

A successful embedding of lipid nanodispersions with high contents was achieved in this study. PVA proved to be a suitable film-forming matrix for ODFs, allowing both lipid nanosuspensions and nanoemulsions to be embedded with a lipid content of 40 wt.% and 47 wt.%, respectively. Lactose was the most suitable matrix for embedding lipid nanodispersions by spray drying, followed by PVA and HPMC. Using a lactose matrix, 45 wt.% nanoparticular oil droplets were loaded into the powders, with a maximum particle size increase of 20 % after powder redispersion. Similar results were obtained for tristearin and tripalmitin particles.

A closer look at how the elongated to platelet-shaped triglycerides are arranged in the ODF matrices using AFM indicated a particle orientation in a stack-like structure, enabling a denser particle packing and resulting in a high lipid load. For the spherical oil droplets, a denser packing was realized indicated by an even 7 wt.% higher embedding capacity, which requires sufficient droplet stabilization against coalescence during the drying process. The AFM images also identified an elongated to platelet-like structure of the tristearin particles embedded in the matrix in the α-modification. The particle shape was confirmed by a more detailed examination

using SEM and the determination of the dimensions of the particles in the initial suspension using AFM. It was assumed that the slow cooling rate and particle stabilization using a polymer and a surfactant led to the newly discovered non-round, but platelet-like particle shape of the metastable tristearin particles in the α-modification.

A closer examination of the particle arrangement in the spray-dried powders revealed an unstructured particle distribution. This is due to the high temperatures to which the lipids are exposed during spray drying, which causes the particles to melt during the drying process, resulting in lipid droplets during spray drying. The particles then recrystallize in the solid matrices. Matrix-dependent recrystallization behavior was observed for trimyristin. While trimyristin nanoparticles are known to form supercooled melts, the particles crystallized directly when embedded in a PVA or HPMC matrix. Liquid trimyristin droplets in the powders were only observed when the lipid was embedded in the lactose matrix, whereas recrystallization was shown during powder storage.

This study also conclusively showed the relevance of AFM imaging for the highly precise analysis of lipid nanocarrier systems embedded in ODFs and powders. The easy and reproducible embedding and sectioning technique introduced in this study altogether enabled facile access to the morphology and distribution of particles inside solid dosage forms by AFM, additionally delivering highly precise z-axis data for subsequent morphology analysis of nanoparticles in suspensions. Compared to standard electron microscopy techniques (TEM, SEM), not only the available z-axis data is highly beneficial to the lipid carrier analysis. Moreover, the missing need of vacuum application in AFM as well as the ability to operate nanoscopic imaging under environmental conditions are further specific advantages allowing efficient analysis of particles embedded in solid dosage forms. Altogether, the applied embedding and imaging techniques of this study can therefore be considered an innovative way to analyze embedded nanocarrier systems and an attractive alternative to commonly employed electron microscopy approaches.

The proven high loading capacity of nanoparticulate lipid carrier systems is a prerequisite for more flexible dosing of lipophilic drugs. Based on this study, future work will focus on loading the lipid carriers with drug candidates and on further processing of the lipid-containing powders into capsules or tablets.

Acknowledgements

D.S. gratefully acknowledges the Rottendorf Foundation for endowing the professorship.

References

[1] C.A.S. Bergstrom, W.N. Charman, C.J.H. Porter, Computational prediction of formulation strategies for beyond-rule-of-5 compounds, Adv. Drug. Deliv. Rev., 101 (2016) 6-21.
[2] H. Bunjes, Lipid nanoparticles for the delivery of poorly water-soluble drugs, J. Pharm. Pharmacol., 62 (2010) 1637-1645.
[3] J. Quodbach, E. Preis, F. Karkossa, J. Winck, J.H. Finke, D. Steiner, Novel Strategies for the Formulation of Poorly Water-Soluble Drug Substances by Different Physical Modification Strategies with a Focus on Peroral Applications, Pharmaceuticals, 18 (2025).
[4] S.B. Lim, A. Banerjee, H. Önyüksel, Improvement of drug safety by the use of lipid-based nanocarriers, J. Control. Release, 163 (2012) 34-45.

[5] Z. Vinarov, B. Abrahamsson, P. Artursson, H. Batchelor, P. Berben, A. Bernkop-Schnurch, J. Butler, J. Ceulemans, N. Davies, D. Dupont, G.E. Flaten, N. Fotaki, B.T. Griffin, V. Jannin, J. Keemink, F. Kesisoglou, M. Koziolek, M. Kuentz, A. Mackie, A.J. Melendez-Martinez, M. McAllister, A. Mullertz, C.M. O'Driscoll, N. Parrott, J. Paszkowska, P. Pavek, C.J.H. Porter, C. Reppas, C. Stillhart, K. Sugano, E. Toader, K. Valentova, M. Vertzoni, S.N. De Wildt, C.G. Wilson, P. Augustijns, Current challenges and future perspectives in oral absorption research: An opinion of the UNGAP network, Adv. Drug. Deliv. Rev., 171 (2021) 289-331.
[6] O.M. Feeney, M.F. Crum, C.L. McEvoy, N.L. Trevaskis, H.D. Williams, C.W. Pouton, W.N. Charman, C.A.S. Bergström, C.J.H. Porter, 50 years of oral lipid-based formulations: Provenance, progress and future perspectives, Adv. Drug. Deliv. Rev., 101 (2016) 167-194.
[7] E. Kupetz, H. Bunjes, Lipid nanoparticles: drug localization is substance-specific and achievable load depends on the size and physical state of the particles, J. Control. Release, 189 (2014) 54-64.
[8] K.D. Stewart, J.A. Johnston, L.S. Matza, S.E. Curtis, H.A. Havel, S.A. Sweetana, H.L. Gelhorn, Preference for pharmaceutical formulation and treatment process attributes, Patient Prefer. Adherence, 10 (2016) 1385-1399.
[9] S. Benita, M.Y. Levy, Submicron emulsions as colloidal drug carriers for intravenous administration: Comprehensive Physicochemical Characterization, J. Pharm. Sci., 82 (1993) 1069-1079.
[10] A. Gupta, Nanoemulsions, Nanoparticles for Biomedical Applications, (2020), 371-384.
[11] K.L. Christensen, G.P. Pedersen, H.G. Kristensen, Preparation of redispersible dry emulsions by spray drying, Int. J. Pharm., 212 (2001) 187-194.
[12] D. Steiner, L.V. Schumann, H. Bunjes, Processing of Lipid Nanodispersions into Solid Powders by Spray Drying, Pharmaceutics, 14 (2022) 2464.
[13] D. Steiner, M. Tidau, J.H. Finke, Embedding of Poorly Water-Soluble Drugs in Orodispersible Films-Comparison of Five Formulation Strategies, Pharmaceutics, 15 (2022) 17.
[14] D. Steiner, J.F. Emmendörffer, H. Bunjes, Orodispersible Films: A Delivery Platform for Solid Lipid Nanoparticles?, Pharmaceutics, 13 (2021) 2162.
[15] J. Sitterberg, A. Ozcetin, C. Ehrhardt, U. Bakowsky, Utilising atomic force microscopy for the characterisation of nanoscale drug delivery systems, Eur. J. Pharm. Biopharm., 74 (2010) 2-13.
[16] T.M. Ho, F. Abik, K.S. Mikkonen, An overview of nanoemulsion characterization via atomic force microscopy, Crit. Rev. Food Sci. Nutr., 62 (2022) 4908-4928.
[17] V. Klang, N.B. Matsko, C. Valenta, F. Hofer, Electron microscopy of nanoemulsions: an essential tool for characterisation and stability assessment, Micron, 43 (2012) 85-103.
[18] J. Wang, J. Zhang, S. Li, D. Liu, A. Bhambhani, H. Zeng, Characterization of structures and molecular interactions of RNA and lipid carriers using atomic force microscopy, Adv. Colloid. Interface Sci., 313 (2023) 102855.
[19] J. Mazuryk, T. Deptuła, A. Polchi, J. Gapiński, S. Giovagnoli, A. Magini, C. Emiliani, J. Kohlbrecher, A. Patkowski, Rapamycin-loaded solid lipid nanoparticles: Morphology and impact of the drug loading on the phase transition between lipid polymorphs, Colloids Surf. A: Physicochem. Eng. Asp., 502 (2016) 54-65.
[20] C. Preetz, A. Hauser, G. Hause, A. Kramer, K. Mader, Application of atomic force microscopy and ultrasonic resonator technology on nanoscale: distinction of nanoemulsions from nanocapsules, Eur. J. Pharm. Sci., 39 (2010) 141-151.
[21] E.M.C. Alexandre, R.V. Lourenço, A.M.Q.B. Bittante, I.C.F. Moraes, P.J.d.A. Sobral, Gelatin-based films reinforced with montmorillonite and activated with nanoemulsion of ginger essential oil for food packaging applications, Food Packaging and Shelf Life, 10 (2016) 87-96.

[22] P. Shahgaldian, L. Quattrocchi, J. Gualbert, A.W. Coleman, P. Goreloff, AFM imaging of calixarene based solid lipid nanoparticles in gel matrices, Eur. J. Pharm. Biopharm., 55 (2003) 107-113.
[23] K. Bharti, P. Mittal, B. Mishra, Formulation and characterization of fast dissolving oral films containing buspirone hydrochloride nanoparticles using design of experiment, J. Drug Deliv. Sci. Technol., 49 (2019) 420-432.
[24] D. Sen Karaman, G. Patrignani, E. Rosqvist, J.H. Smatt, A. Orlowska, R. Mustafa, M. Preis, J.M. Rosenholm, Mesoporous silica nanoparticles facilitating the dissolution of poorly soluble drugs in orodispersible films, Eur. J. Pharm. Sci., 122 (2018) 152-159.
[25] S. Czyz, M. Wewers, J.H. Finke, A. Kwade, B. van Eerdenbrugh, M. Juhnke, H. Bunjes, Spray drying of API nanosuspensions: Importance of drying temperature, type and content of matrix former and particle size for successful formulation and process development, Eur. J. Pharm. Biopharm., 152 (2020) 63-71.
[26] P.F. Yue, Y. Li, J. Wan, M. Yang, W.F. Zhu, C.H. Wang, Study on formability of solid nanosuspensions during nanodispersion and solidification: I. Novel role of stabilizer/drug property, Int. J. Pharm., 454 (2013) 269-277.
[27] Councile of Europe, European Pharmacopeia, European Directorate for the Quality of Medicines and Healthcare, Strasbourg, France, 2023.
[28] T.M. Dreher, J. Glass, A.J. O'Connor, G.W. Stevens, Effect of rheology on coalescence rates and emulsion stability, AIChE Journal, 45 (1999) 1182-1190.
[29] R.F. Ribeiro, M.H. Motta, A.P.G. Harter, F.C. Flores, R.C.R. Beck, S.R. Schaffazick, C. de Bona da Silva, Spray-dried powders improve the controlled release of antifungal tioconazole-loaded polymeric nanocapsules compared to with lyophilized products, Mater Sci. Eng. C Mater. Biol. Appl., 59 (2016) 875-884.
[30] M. Wewers, S. Czyz, J.H. Finke, E. John, B. Van Eerdenbrugh, M. Juhnke, H. Bunjes, A. Kwade, Influence of Formulation Parameters on Redispersibility of Naproxen Nanoparticles from Granules Produced in a Fluidized Bed Process, Pharmaceutics, 12 (2020) 363.
[31] J.R. Jørgensen, W. Mohr, M. Rischer, A. Sauer, S. Mistry, A. Müllertz, T. Rades, Stability and intrinsic dissolution of vacuum compression molded amorphous solid dispersions of efavirenz, Int. J. Pharm., 632 (2023).
[32] H. Wen, K.R. Morris, K. Park, Synergic Effects of Polymeric Additives on Dissolution and Crystallization of Acetaminophen, Pharm. Res., 25 (2007) 349-358.
[33] M.L. Taboada, T. Heiden-Hecht, M. Brückner-Gühmann, H.P. Karbstein, S. Drusch, V. Gaukel, Spray drying of emulsions: Influence of the emulsifier system on changes in oil droplet size during the drying step, J. Food Process. Preserv., 45 (2021).
[34] S. Joseph, M. Rappolt, M. Schoenitz, V. Huzhalska, W. Augustin, S. Scholl, H. Bunjes, Stability of the Metastable alpha-Polymorph in Solid Triglyceride Drug-Carrier Nanoparticles, Langmuir, 31 (2015) 6663-6674.
[35] S. Gehrer, M. Schmiele, M. Westermann, F. Steiniger, T. Unruh, Liquid crystalline phase formation in suspensions of solid trimyristin nanoparticles, J. Phys. Chem. B, 118 (2014) 11387-11396.
[36] M. Schmiele, T. Schindler, M. Westermann, F. Steiniger, A. Radulescu, A. Kriele, R. Gilles, T. Unruh, Mesoscopic structures of triglyceride nanosuspensions studied by small-angle X-ray and neutron scattering and computer simulations, J. Phys. Chem. B, 118 (2014) 8808-8818.
[37] H. Bunjes, K. Westesen, M.H.J. Koch, Crystallization tendency and polymorphic transitions in triglyceride nanoparticles, Int. J. Pharm., 129 (1996) 159-173.
[38] K.M. Rosenblatt, H. Bunjes, Poly(vinyl alcohol) as emulsifier stabilizes solid triglyceride drug carrier nanoparticles in the Alpha-modifikation, Mol. Pharm., 6 (2008) 105-120.

[39] M. Schoenitz, S. Joseph, A. Nitz, H. Bunjes, S. Scholl, Controlled polymorphic transformation of continuously crystallized solid lipid nanoparticles in a microstructured device: a feasibility study, Eur. J. Pharm. Biopharm., 86 (2014) 324-331.
[40] H. Bunjes, M.H.J. Koch, K. Westesen, Influence of emulsifiers on the crystallization of solid lipid nanoparticles, J. Pharm. Sci., 92 (2003) 1509-1520.
[41] A. Ziaee, A.B. Albadarin, L. Padrela, T. Femmer, E. O'Reilly, G. Walker, Spray drying of pharmaceuticals and biopharmaceuticals: Critical parameters and experimental process optimization approaches, Eur. J. Pharm. Biopharm., 127 (2019) 300-318.
[42] N. Fan, Z. He, P. Ma, X. Wang, C. Li, J. Sun, Y. Sun, J. Li, Impact of HPMC on inhibiting crystallization and improving permeability of curcumin amorphous solid dispersions, Carbohydr. Polym., 181 (2018) 543-550.
[43] L.K. Mueller, L. Halstenberg, N. Di Gallo, T. Kipping, Evaluation of a Three-Fluid Nozzle Spraying Process for Facilitating Spray Drying of Hydrophilic Polymers for the Creation of Amorphous Solid Dispersions, Pharmaceutics, 15 (2023).
[44] Y. Roos, Melting and glass transition of low molecular weight carbohydrates, Carbohydr. Res., 238 (1993) 39,48.
[45] A. Illing, T. Unruh, Investigation on the flow behavior of dispersions of solid triglyceride nanoparticles, Int. J. Pharm., 284 (2004) 123-131.
[46] H. Bunjes, Structural properties of solid lipid based colloidal drug delivery systems, Cur. Opin. Colloid Interface Sci., 16 (2011) 405-411.
[47] A. Gordillo-Galeano, C.E. Mora-Huertas, Solid lipid nanoparticles and nanostructured lipid carriers: A review emphasizing on particle structure and drug release, Eur. J. Pharm. Biopharm., 133 (2018) 285-308.
[48] H. Bunjes, F. Steiniger, W. Richter, Visualizing the Structure of Triglyceride Nanoparticles in Different Crystal Modifications, Langmuir, 23 (2007) 4005-4011.
[49] M. Schmiele, S. Gehrer, M. Westermann, F. Steiniger, T. Unruh, Formation of liquid crystalline phases in aqueous suspensions of platelet-like tripalmitin nanoparticles, J. Chem. Phys., 140 (2014).

Graphical Abstract